

Custom Distribution for Sampling-Based Motion Planning

Gabriel O. Flores-Aquino¹ · J. Irving Vasquez-Gomez^{2,3} · Octavio Gutierrez-Frias¹

Received: date / Accepted: date

Abstract Sampling-based algorithms are widely used in robotics because they are very useful in high dimensional spaces. However, the rate of success and quality of the solutions are determined by an adequate selection of their parameters such as the distance between states, the local planner, and the sampling method. For robots with large configuration spaces or dynamic restrictions selecting these parameters is a challenging task. This paper proposes a method for improving the results for a set of the most popular sampling-based algorithms, the Rapidly-exploring Random Trees (RRTs) by adjusting the sampling method. The idea is to replace the sampling function, traditionally a Uniform Probability Density Function (U-PDF) with a custom distribution (C-PDF) learned from previously successful queries of a similar task. With few samples, our method builds the custom distribution allowing a higher success rate and sparser trees in randomly new queries. We test our method in several common tasks of autonomous driving such as parking maneuvers or obstacle clearance and also in complex scenarios outperforming the base orig-

inal and bias RRT. In addition, the proposed method requires a relative small set of examples, unlike current deep learning techniques that require a vast amount of examples.

Keywords sampling-based motion planning · RRTs · bias sampling · autonomous vehicle · autonomous parking

1 Introduction

The motion planning problem from a robotics perspective has the goal of determining the set of inputs for an open-loop control that drives the robot from an initial configuration to a goal configuration in a feasible and collision-free space while the kinematic and dynamic constraints are satisfied. Motion planning has been investigated from different perspectives [14] using techniques such as potential field, neuronal networks [29] or genetic algorithms [30], to name a few. In particular, we are interested in motion planning for automated vehicles where the problem has been addressed from formal approaches like control theory [27] to a machine learning problem. For a complete review of techniques the reader is referred to [26]. However, in the last decades, the attention has been focused on sampling-based motion planners (SBMP) due to their simplicity and functionality even in high dimensional spaces [24]. For sampling-based methods, there are two main approaches, the single-query models and multi-query models for example the rapidly exploring random tree (RRT) and the probabilistic roadmap (PRM) respectively. From this point, a great variety of ideas emerged to cover the weak aspects to improve the quality of the solutions or reduce the computational expense. A good example is the RRT* variation [12] where the solution

Gabriel O. Flores-Aquino
E-mail: gflores0500@alumno.ipn.mx

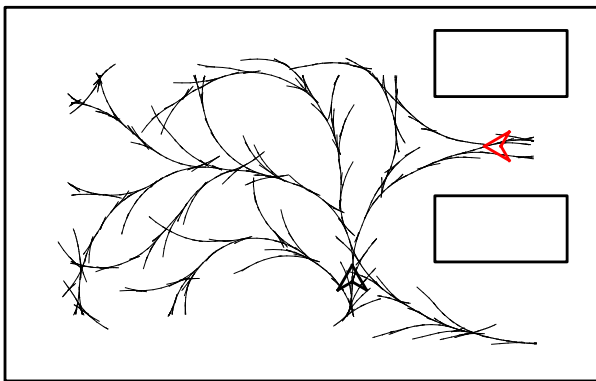
J. Irving Vasquez-Gomez
E-mail: jvasquezg@ipn.mx

O. Octavio Gutierrez-Frias
E-mail: ogutierrezf@ipn.mx

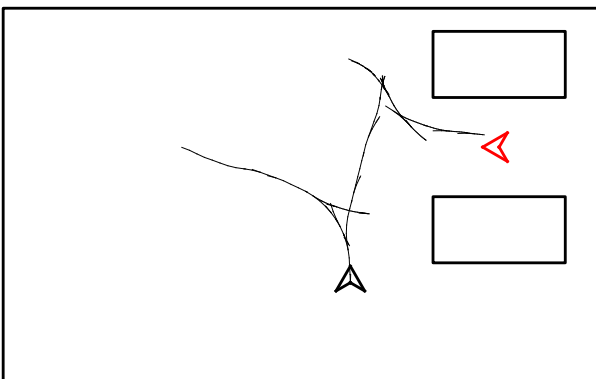
¹Instituto Politécnico Nacional (IPN), Sección de Estudios de Posgrado e Investigación de la Unidad Profesional Interdisciplinaria en Ingeniería y Tecnologías Avanzadas (UPIITA), Ciudad de México, México

² Instituto Politécnico Nacional (IPN), Centro de Innovación y Desarrollo Tecnológico en Cómputo (CIDETEC), Ciudad de México, México

³Consejo Nacional de Ciencia y Tecnología (CONACYT) Ciudad de México, México



stg:2, test:11, PDF:uniform, vertices= 3128



stg:2, test:11, PDF:custom, vertices= 318

Fig. 1 Results of a tree-based graph for parallel parking. Top row, tree that samples from a uniform distribution (U-PDF). Bottom row, tree that samples from the proposed custom distribution (C-PDF). Black triangle indicates starting configuration. Red triangle indicates goal configuration. Fig. best seen in color.

converges to the optimum and more recently the SST method [10] that produces sparse trees or FMT* for complex motion planning problems [28]. Other works have been focused on improving the parameters to tune the algorithm; recent examples of this approach are the use of reinforcement learning to complement aspects like the space of metric, the local planner strategy [6], [13] or the distribution of probability [7] unfortunately these approaches require a very large number of examples to infer knowledge. Nevertheless, we share the enthusiasm of exploring the cross-field between motion planning and machine learning. Some works in this new field are proposed in [29] where is present a neural planner and [25], where a the planning process is realized in a learning plannable representation in a reduced configuration space.

This paper focuses on exploring the way by which the planner samples the configuration space. In this sense, typically a uniform distribution is the first option be-

cause it produces a graph or roadmap that spans evenly over the free configuration space but with this approach arise some troubles. For example in planners such as PRM; a uniform distribution has a poor performance in environments where there are narrow passages because this regions are difficult to sample. To solve the aforementioned problem, some techniques oversample such passages, e.g. the bridge test [9], which allows refining the connectivity in narrow passages or the Gaussian sampling strategy [15], [8], whose objective is to obtain a model of the free configuration spaces, including these difficult passages; other approaches focuses on extracting local characteristic from the workspace for bias the sampling [17], [18], [19]. These hybrid sampling strategies are appropriate for planners with a multi-query model like PRM because they are helpful to maintain a roadmap connected, and this offers the possibility of reusing the roadmap for a different group of queries. But for a single-query model may not be practical because each query needs to create a new graph hence covering the complete workspace can be unnecessary, while it's more important to achieve a high rate of convergences and low computational time. For this reasons, it is very important to explore new forms to efficiently sample the configuration space when a small dataset of examples is available.

For a single-query model like RRT or any tree-based algorithm, the traditional approach consists of sampling the space randomly with a uniform distribution and grown the tree iteratively until the goal is reached. One technique to improve the results can be to find a method for guiding the tree growth. For example, in [16] and [20], the tree is guided by selecting the option of expansion with maximal expected utility but, this type of method modifies the structure of the algorithm, which can be hard to implement. In this sense, other works, as [21] and [23], reuse the found paths by developing a framework to improve the performance respect the computing time.

The present work uses previous knowledge to improve the sampling function assuming that exist a better PDF for each environment. We focuses on tuning the probability density function used in the sampling method such that we can build sparser trees and at the same time we increase the success rate with relatively few samples, as shows the Figure 1. More over, we are interested in guiding the tree by only tuning the settings without making modifications to the algorithm structure and, to do this, we utilize the prior knowledge acquired from previous experience. We compare our method versus the classic version of RRT with a uniform distribution and versus a RRT version with the

distribution skewed by the target configuration (RRT goal bias). We show that our method generates directed trees that are especially useful in environments where the robot has a similar goal but its initial configuration varies. For this reason, the proposed experiments are common tasks for autonomous driving cars; like autonomous parking and evasive maneuvers. Our method minimizes the effects of a not well-adapted sampling domain and has significant improvement over classic RRT. In addition our results provide evidence that the method can be applicable across other planners or robotic platforms.

The rest of the paper is organized as follows. In section 2, we present the generality of RRT algorithm and its parameters for the three proposed environments. In section 3, we make the description of the method and, in section 4, we present the numerical results about using the C-PDF compared against the classic RRT goal and bias versions. Finally in section 5, we present the conclusions and future work.

2 Theoretical background

This section briefly describes the RRT algorithm and its parameters such as the robot model, the distance metric and the environment for the proposed tasks.

2.1 Rapidly-exploring random trees

Sampling-based motion planning is a set of incremental sampling and searching algorithms. Which target is to avoid the explicit construction of the obstacle space \mathcal{C}_{obs} and to explore the state space \mathcal{C}_{space} with a sampling scheme [1]. Two of the most widely used sampling-based algorithms are Probabilistic Road Maps (PRM)[4] and Rapidly-exploring Random Trees [24]. RRT it's a special case of the family referred to as rapidly exploring Dense Trees (RDTs); these algorithms have a dense covering of the \mathcal{X}_{space} , and this feature allows them to be probabilistically complete. The goal is to build a topological graph denoted by $\mathcal{G}(V, E)$ where each vertex V is a configuration, and each edge E is a path that connects two vertices inside the free space $\mathcal{X}_{free} = \mathcal{X}_{space} \setminus \mathcal{X}_{obs}$ [1]. Unlike PRM, the RRT follows a single-query model, for each query (q_I, q_G) , robot model and obstacle set, the planner returns a topological graph or a tree-based graph and whether the query was successful, a branch of the tree is a path to the goal configuration q_G . In short, the RRT algorithm follows the steps [1]:

- Initialization
- Vertex Selection Method (VSM)

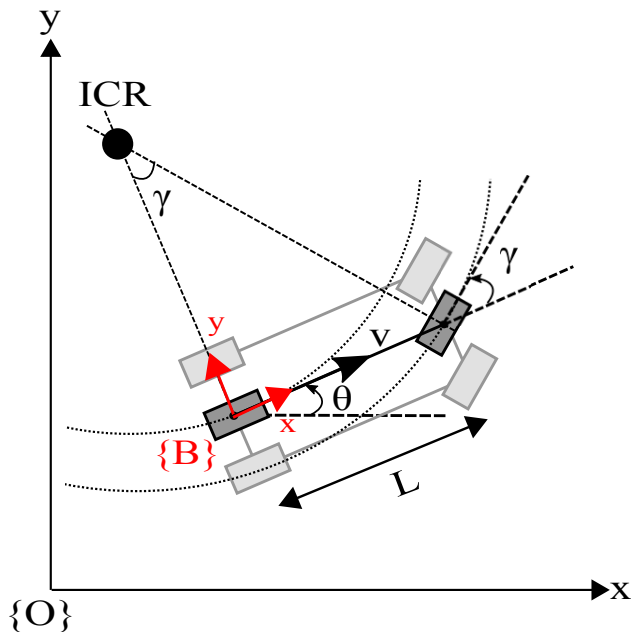


Fig. 2 Kinematic model of a car. The world frame $\{O, x, y\}$ in color black. The body frame $\{B, x, y\}$. ICR denotes the Instantaneous Center of Rotation and L the distance between wheels axles.

- Local Planing Method (LPM)
- Graph update
- Check for solution
- Return to VSM

The VSM consist in generating a random vertex, q_{rand} between the proposed lower and upper state and finding the nearest existing vertex, q_{near} , according to the metric space then, if this vertex is an element of the free state space \mathcal{X}_{free} and satisfies the conditions of LPM, this vertex is added to the tree like a new vertex, q_{new} . If the method reaches a solution returns true and the algorithm finish, in other case, returns to the VSM, this process is repeated for k iterations.

2.2 Robot model

We define the State Transition Equation (STE) using the kinematic model of car-like configuration, see Figure 2, described by the non-linear ordinary differential equation (1).

$$\dot{X} = f(x, u) = \begin{bmatrix} \dot{x} \\ \dot{y} \\ \dot{\theta}_y \end{bmatrix} = \begin{bmatrix} v \cos(\theta_y) \\ v \sin(\theta_y) \\ v \frac{\tan(\gamma)}{L} \end{bmatrix} \quad (1)$$

Let \mathcal{X} denoted the space state and $x \in \mathcal{X}$ such that $\hat{x} = (q, \dot{q})$ where q is the set of generalized coordinates defined by the variables x and y for the position on the plane and θ_y for the orientation around the z -axis such that represents the robot in a $2D$ workspace. This model is suitable for tasks that involve a low velocity of translation where it is not necessary considerate a tire model. From equation (1) the variable u represents the robot input such that $u \in U$. See equation (2).

$$u = \{v, \gamma\} \quad (2)$$

Where v is the translational velocity and, γ is the steering angle applied to the front tires. It's important to point out that a car-like vehicle has the non-holonomic constraint $\dot{y}\cos(\theta) - \dot{x}\sin(\theta) \equiv 0$ the which limits its ability to move in an arbitrary direction [3], this characteristic makes difficult some tasks like parking manoeuvres.

2.3 Distance metric

To determine the similarity between two states $X_1 = \{x_1, y_1, \theta_1\}$ and $X_2 = \{x_2, y_2, \theta_2\}$, we propose a normalized metric ρ defined by the equation (3).

$$\rho = \omega_1\rho_1 + \omega_2\rho_2 \quad (3)$$

where the sub-metrics ρ_1 and ρ_2 determine the similarity between position and orientation equation (4) and (5) respectively. The variables ω_1 and ω_2 weigh the sub-metrics for each of the proposed tasks and, they are statistically determined in every environment. In this case for task 1 and 4 $\omega_1 = 0.8$, $\omega_2 = 0.2$ and for task 2 and 3 $\omega_1 = 0.9$, $\omega_2 = 0.1$.

$$\rho_1 = \left(\frac{(x_2 - x_1)^2 + (y_2 - y_1)^2}{(x_{max} - x_{min})^2 + (y_{max} - y_{min})^2} \right)^{\frac{1}{2}} \quad (4)$$

$$\rho_2 = \frac{\min(\text{abs}(\theta_1 - \theta_2), 2\pi - \text{abs}(\theta_1 - \theta_2))}{\pi} \quad (5)$$

3 Custom sampling distribution

In this section, we propose a methodology for constructing a custom probability density function (C-PDF) that will be used by the planner in order to improve its performance. The methodology consists in executing the RRT planner for an initial query that we denominated the construction query. If the construction query produces a successful path, then we collect specific data

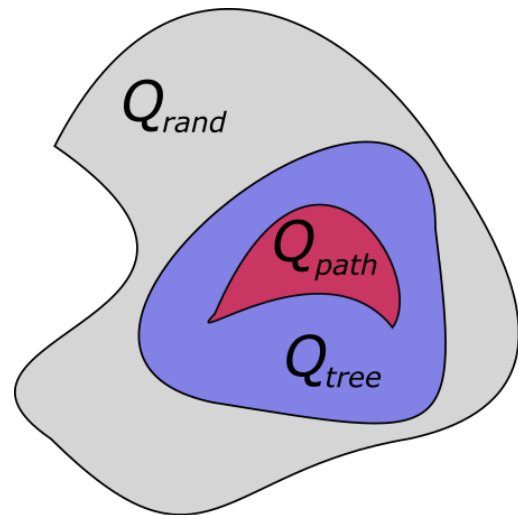


Fig. 3 Venn diagram of sampling regions. In color gray the set of all random vertices Q_{rand} , in color purple the sub-set of random vertices that contribute to generate the tree, Q_{tree} and in color red only the random vertices that contribute to a path that resolve the query, Q_{path} .

from the sampling space; in another case, we discard these results. We repeat this process until reaching m samples to approximate a C-PDF. Finally, we use this function together with the rejection sampling method [2] as sampling source in a new set of queries improving the planner performance. In section 3.1, we expose the details of this process taking the environment of the task 1 as example and in the section 3.2 we explain the details of the sampling method.

3.1 Collecting data

We know that a uniform distribution \mathcal{P} covers the workspace evenly. In ideal conditions each random vertex (q_{rand}) should generate a new vertex (q_{new}) for the topological graph \mathcal{G} but for different reasons only a reduced percentage of q_{rand} samples produces a q_{new} vertex, we denominated this sub-set of q_{rand} as Q_{tree} . If the query is successful within \mathcal{G} there is a branch that solves the query. This branch or path has n vertices and each one of this vertices has a corresponding element within of set Q_{rand} . Therefore, the sub-set of Q_{rand} , which contains the random vertex that supported the tress, is $Q_{tree} \subseteq Q_{rand}$ and the sub-set that supported the path is defined as $Q_{path} \subseteq Q_{tree}$, as shows Figure 3.

If we collect only Q_{path} in the test, we can notice that these vertices follow a different distribution compared with the original \mathcal{P} and this trend continues with each new test for the same query, this process can be

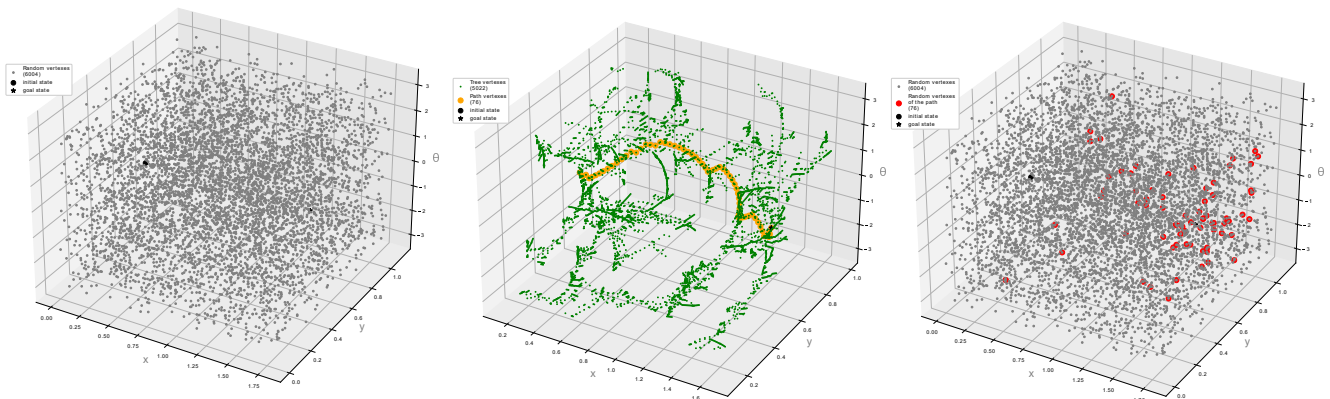


Fig. 4 From \mathcal{P} distribution the random vertices in the state space. From left to right. All the random vertices in gray. The tree vertices in green and the the solution path in orange. The random vertices are painted in gray and in red the random vertices that generated the path, Q_{path} .

seen in Figure 4. With the objective of inferring the shape of \mathcal{C} distribution, we need to collect a significant number of samples from Q_{path} . To do this we repeat this process until reaching m samples, For the task 1, we collected 541 samples in 8 queries. In this case, the state space is of equal dimension to \mathcal{C}_{space} and the total of the samples and their distribution for the three stages can be seen in Figure 5. This collection process is summarized in Algorithm 1. Where the output is the set \mathcal{S} that denotes the set of m vertices Q_{path} . Let \mathcal{G} denote the topological graph formed for vertices and edges, Q_{new} denotes the set of all the random vertices that contribute to the graph, Q_{rand} denotes the set of all the random vertices and \mathcal{P} denotes the set of all vertices for the path. Let $GENERATE_RRT$ denote the RRT path planning described in Algorithm 2 and $RESOLVE_QUERY$ the method to find a path within \mathcal{G} . Please note that algorithm 2 is proposed in [24], we only add a pair of simple modifications highlighted in gray to save and return the topological graph together with the sets Q_{rand} and Q_{new} .

The line 5 in $COLLECTING_DATA$ uses the topological graph \mathcal{G} along with the initial and goal configuration as inputs for the function $RESOLVE_QUERY$ to find the path \mathcal{P} . Finally if \mathcal{P} is a not empty we track and save the vertices Q_{path} from Q_{rand} , lines 7 to 12. The process continue until reaching m samples.

3.2 Sampling data from the custom distribution

We use the rejection sampling method to generate samples q_{rand} with the shape of the C-PDF formed by the set \mathcal{S} . The set \mathcal{S} is in the state space for this case formed

Algorithm 1: COLLECTING_DATA()

Parameters: k, Δ_t, m

Input : q_{init}, q_{goal}

Output : \mathcal{S}

```

1  $\mathcal{S} \leftarrow \emptyset$ ;
2 while  $\mathcal{S} < m$  do
3    $\mathcal{G}, Q_{rand}, Q_{new} \leftarrow \emptyset$ ;
4    $\mathcal{G}, Q_{rand}, Q_{new} \leftarrow GENERATE\_RRT(q_{init}, k, \Delta_t)$ ;
5    $\mathcal{P} \leftarrow RESOLVE\_QUERY(q_{init}, q_{goal}, \mathcal{G})$ ;
6   if  $\mathcal{P} \neq \emptyset$  then
7     for  $i = 0$  to  $\mathcal{P}$  do
8       if  $\mathcal{P} \in Q_{new}$  then
9          $\mathcal{S} \leftarrow \mathcal{S} \cup Q_{rand}(Q_{new}(\mathcal{P}))$ 
10      end
11    end
12  end
13 end
14 Return  $\mathcal{S}$ 

```

with three variables x, y, θ . In order to find the C-PDF we need express this variables in a normalized space denominated sampling space. For this purpose, we use the equation 6.

$$r_{m,i} = \frac{\mathcal{S}_{m,i} - LS_i}{US_i - LS_i} \quad (6)$$

The sub-script i iterate between each variable of configuration x, y and θ , the sub-script m iterate between each element of the set \mathcal{S} ; LS and US are the lower and upper limits in the X_{space} for each variable. Applying the equation 6 to each element, we obtain the sampling space r_x, r_y and r_θ these are correlated random variables but to simplify the model, for task 1 to 3 we express them like three independent random variables and discretized in ten bins to generate the

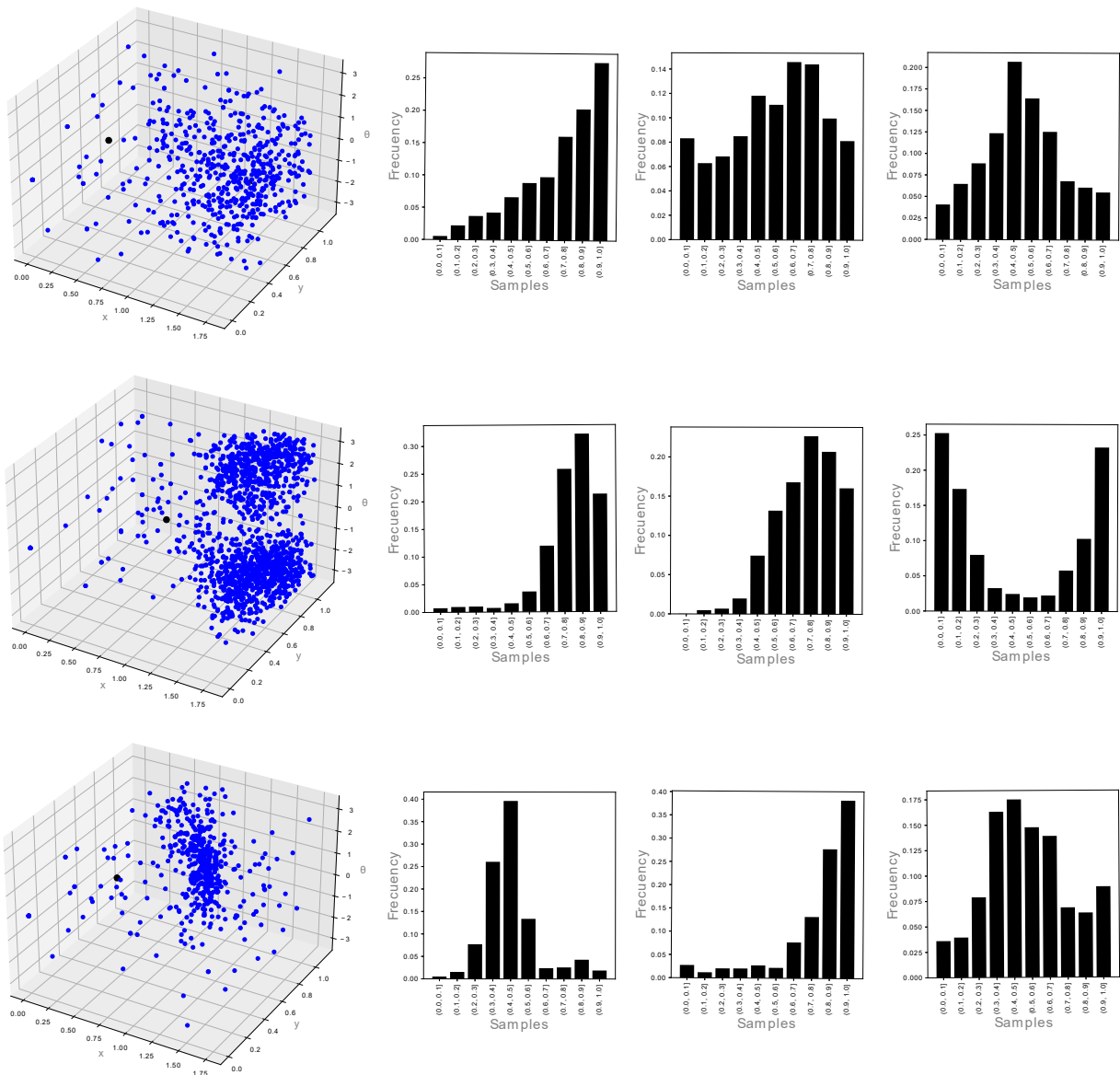


Fig. 5 Set \mathcal{S} for task 1 to 3 from left to right and top to bottom. In color blue the set \mathcal{S} in the state space and in black their histogram for independent variables $\{x, y, \theta\}$.

histograms of Figure 5. For the task 4 we consider the correlation, see Figure 8. Following, we use the rejection sampling method [2] to generate the C-PDF into the parameters of the planner. The idea of this method is sampling a target distribution $p(z)$ usually normalized from a more simple distribution $q(z)$ denominated proposal distribution. To apply the method we need to propose a scaling constant c such that $p(z) \leq c q(z)$ i.e. the scaling proposal distribution covers the target distribution over the range of z . The next step is to generate a random number z_0 from the scaled proposal distribution and to propose a candidate sample u_0 in the interval $[0, c q(z_0)]$ if the $u_0 \leq p(z_0)$ then the sample

is accepted in other case is rejected. For a detailed explanation the reader is referred to [2]. We implemented a discrete version of this method using a uniform distribution as proposal distribution and each one of the distributions formed by r_x, r_y, r_z as target distribution.

4 Experiments

For the evaluation, first we proposed three scenarios with the same conditions but with a different distribution of X_{obs} . Each environment was selected because it is a common task in the autonomous driving scene. In this tasks we evaluated the performance for the con-

Algorithm 2: GENERATE_RRT($x_{init}, K, \Delta t$)

```

1  $\mathcal{G}.init(q_{init});$ 
2 for  $k = 1$  to  $K$  do
3    $q_{rand} \leftarrow RANDOM\_STATE();$ 
4    $\mathcal{Q}_{rand} = \mathcal{Q}_{rand} \cup q_{rand};$ 
5    $q_{near} \leftarrow NEAREST\_NEIGHBOR(q_{rand}, \mathcal{G});$ 
6    $u \leftarrow SELECT\_INPUT(q_{rand}, q_{near});$ 
7    $q_{new} \leftarrow NEW\_STATE(q_{near}, u, \Delta t);$ 
8    $\mathcal{Q}_{new} = \mathcal{Q}_{new} \cup q_{new};$ 
9    $\mathcal{G}.add\_vertex(q_{new});$ 
10   $\mathcal{G}.add\_edge(q_{near}, q_{new}, u);$ 
11 end
12 Return  $\mathcal{G}, \mathcal{Q}_{rand}, \mathcal{Q}_{new}$ 

```

Car-like robot	
Height	0.197m
Length	0.39m
Width	0.195m
Distance between axis(L)	0.255m
Rear distance to center of gravity	0.14m
Front distance to center of gravity	0.115m
Mass(m)	0.2891kg
Moment of inertia (I_z)	$4.7 \times 10^{-3} \text{kgm}^2$

Table 1 Test robot specifications

struction query and for a set of ten random queries with the same q_{goal} but different q_{init} . In the task 4 we evaluate the method in a more complex environment with narrow passages for three random q_{init} keeping q_{goal} . We describe in sub-section 4.1 the generality of proposed environments. The environments were designed for a test robot of scale 1:10 with the characteristics described in Table 4.

In sub-section 4.2, we describe the metrics used and in the section 4.3, we expose the comparative results between the U-PDF and the C-PDF for the construction query followed by a second series of experiments where we compare the C-PDF with the U-PDF and the RRT goal bias version for a group of ten random queries for task 1 to 3 and a comparative between U-PDF and C-PDF for task 4.

4.1 Proposed tasks

All the tasks are define in \mathcal{W} , such that contains an obstacle region described as $\mathcal{O} \subset \mathcal{W}$. For the first three tasks the lower and upper world coordinates for the \mathcal{C}_{space} are defined as $X_{LS} = \{0.0, 0.0, -\frac{\pi}{2}\}$ for Lower State LS and $X_{US} = \{1.8, 1.125, \frac{\pi}{2}\}$ for Upper State US , see Figure 6 and for the four task $X_{LS} = \{0.0, 0.0, -\frac{\pi}{2}\}$ for Lower State and $X_{US} = \{3.1, 3.1, \frac{\pi}{2}\}$ for Upper State US , see Figure 7. Thereby the proposed tasks are follows:

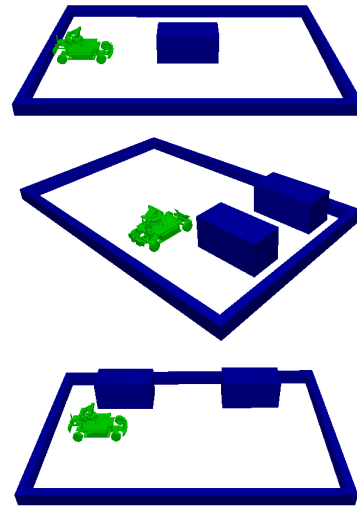


Fig. 6 Representation of the proposed tasks using Motion Planning Library [11]. From top to bottom; avoiding a static obstacle, parallel parking and line parking, respectively. In color blue the obstacles in color white the free work-space and color green the robot.

$u_{1,2,\dots,58}$	$V(m/s)$	$\gamma(deg)$
Stop	0	0
High velocity	0.05	$\{-45, -40, -35, \dots, 40, 45\}$
Low velocity	0.01	$\{-45, -40, -35, \dots, 40, 45\}$
Reverse	-0.01	$\{-45, -40, -35, \dots, 40, 45\}$

Table 2 Set of 56 discrete control inputs for each proposed task. Divided into four sub-categories of velocity.

1. Avoiding a static obstacle: The goal in this task is to avoid a static obstacle that obstructs the route of the car.
2. Parallel parking: Parking in a lot with dimensions $[0.40m, 0.30m]$ and between two rectangular
3. Line parking: Parking in a lot with dimensions $[0.50m, 0.20m]$ and between two rectangular obstacles placed longitudinally.
4. Narrow passages: Resolve a map with narrow passages

In task four, we consider the probabilistic density function in an \mathbb{R}^3 space. Building from a ten random initial configuration and sampled with the rejected method.

Each example used a set of discrete control inputs formed by three inputs sub-set denoted as lower-speed, higher-speed and reverse-speed formed a total of 58 discrete inputs 19 by each sub-set, see table 2. For example, the input number 2 is the pair $u_2 = \{0.05, -45\}$, the input $u_{25} = \{0.01, -25\}$ and in the same way by the consecutive inputs.

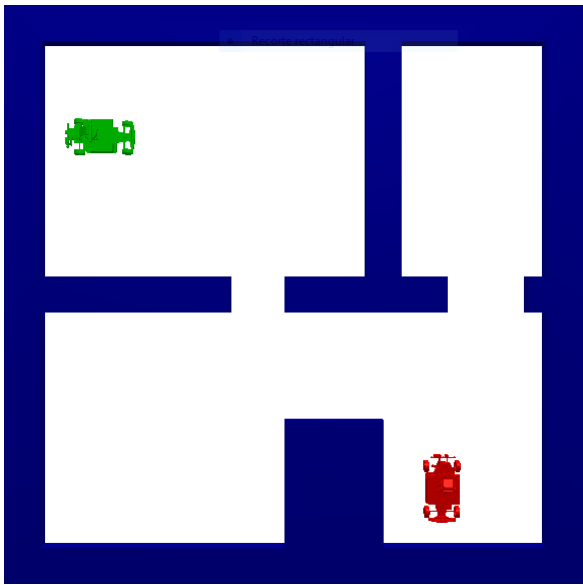


Fig. 7 Task with narrow passages. In color green initial configuration and red color final configuration

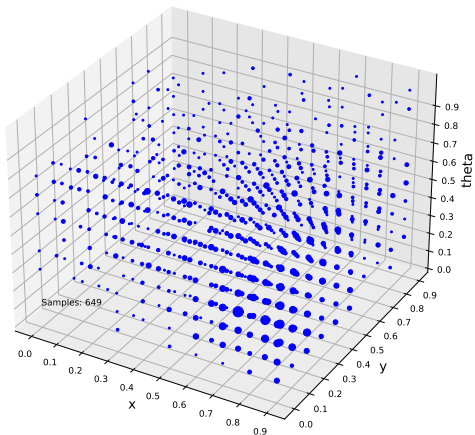


Fig. 8 FDP for task 4. In color blue the sphere which radius represent the amount of samples

4.2 Performance metrics

To evaluate the performance of our method we utilized the next four metrics:

1. Tree density: The number of vertices of the tree-based graph.
2. Connectivity percentage: The percentage of iterations that produces and connect a new vertex.
3. Vertices in the path: The amount of vertices for the solution path.

Construction query				
PDF	Tree Density	Connectivity percentage	Vertices in path	Success rate
Task 1				
U-PDF	2,336.41	0.87	67.66	0.45
C-PDF	1,093.0	0.79	70.96	0.55
Task 2				
U-PDF	3,313.68	0.68	121.68	0.60
C-PDF	336.25	0.65	137.5	1.0
Task 3				
U-PDF	4,679.0	0.65	67.83	0.45
C-PDF	383.75	0.61	57.9	1.0

Table 3 The table shows comparative results between U-PDF versus C-PDF for the construction query. Each numerical value is the arithmetic average before twenty tests. The best results are highlighted in gray

4. Success rate: The percentage of queries that find a solution within a limit of 10,000 cycles.

4.3 Experiments analysis

For the first three tasks we present in Table 3 the results using a U-PDF versus a C-PDF for the construction query. In Table 4 the results using a U-PDF and GB-PDF versus a C-PDF for a set of random queries.

Results for construction query

We use the results of the construction query as a reference for expected performance and the random queries for validate that the method is useful for different configurations. We can observe from Table 3 that the U-PDF generates less dense trees; for example, for the parallel parking, task 2, the number of vertices decreases by 89.85%; this trend continues for other environments, although to a lesser extend. Another relevant issue is the increase in the success rate. For example while for the task 1 with U-PDF, we have 0.45 of likelihood to obtain a successful test, with the same parameters only change the PDF, the likelihood increase by 0.1 and for the other two environments the increase is much higher rising to the maximum likelihood. For the items, connectivity percentage and vertices in path the results are practically the same with U-PDF or C-PDF, but in general C-PDF present an increase in vertices and decrease in connectivity. In Figure 9, we presented representative examples for these results in terms of the tree-based graph. The results for the construction query prove that the C-PDF improves the performance of the RRT respect to U-PDF; however, we expect this results because we constructed this distribution for that explicit query. Now the question is to know if this C-PDF remain useful with a new set of queries.

Random query					
PDF	Tree Density	Connectivity percentage	Vertices in path	Path in meters	Success rate
Task 1					
U-PDF	7041.60	0.83	73.60	1.02	0.26
GB-PDF	3718.40	0.59	85.35	1.06	0.53
C-PDF	4152.63	0.79	78.62	0.92	0.60
Task 2					
U-PDF	4638.13	0.65	164.04	1.43	0.53
GB-PDF	2543.70	0.47	165.50	1.15	0.66
C-PDF	570.26	0.38	216.45	1.51	0.96
Task 3					
U-PDF	4665.66	0.65	114.43	1.33	0.50
GB-PDF	2493.30	0.49	144.74	1.43	0.66
C-PDF	1224.16	0.48	189.45	1.61	0.96
Task 4					
U-PDF	6265.13	0.70	110.00	2.65	0.20
GB-PDF	4064.86	0.50	202.20	3.29	0.36
C-PDF	5030.46	0.72	151.05	2.80	0.46

Table 4 The table shows comparative results between U-PDF, GB-PDF and C-PDF for a group of ten random queries for task 1 to 3 and three random queries for task 4. For each task the best results are highlighted in color gray.

Results for random queries

For this propose, we generated a set of random q_I , and retain the same q_G . We show the comparative results for the random queries in each scenario with a U-PDF, GB-PDF and C-PDF in the Table 4. We summarized the result below:

- Increase the success rate by +100% with respect to U-PDF and +34% with respect to goal bias RRT version.
- The density of the tree-based graph decreases by -50.86% with respect to U-PDF and -14.38% with respect to goal bias RRT version.

This results imply a tree-based graph less dense, therefore enhancing the computational time. We also have a considerable increase in the probability of success when making a query. This advantages are important because a robot in real operation need plan in a short time. On the other hand, we have some negative consequence when using the C-PDF summarized as:

- Connectivity decrease by -15% with respect to U-PDF but increase +15% with respect to goal bias RRT version.
- Increase the vertex in the path by +37% with respect to U-PDF and +11% with respect to goal bias RRT version.

For the task four with narrow passage you can see the trend for create sparse trees while the success rate increase in Figure 10.

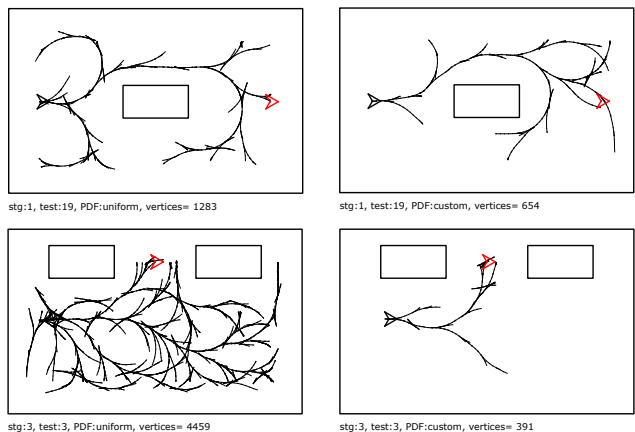


Fig. 9 Results of a tree-based graph for the construction query. Left column, tree with U-PDF and right column, tree with C-PDF.

The loss of connectivity and the increase of the number of vertexes in the path are natural consequences of having a skewed distribution due to loss of variety in the generation of random vertexes. However, for the connectivity is important don't have an excessive loss in order to reduce the computing time. The results show that our method has a better connectivity than the goal bias version although worst that the U-PDF but this increase is not significant since we have sparse trees. For the path measure we only considerer, by obvious reason the successful queries. In the table 4 we presented the distance path measure in terms of the number of vertexes and in distance traveled in meters. In general fewer vertexes meaning fewer control actions, therefore, save energy. Our custom distribution presents a considerable increase respect to a U-PDF (+37%) in terms of

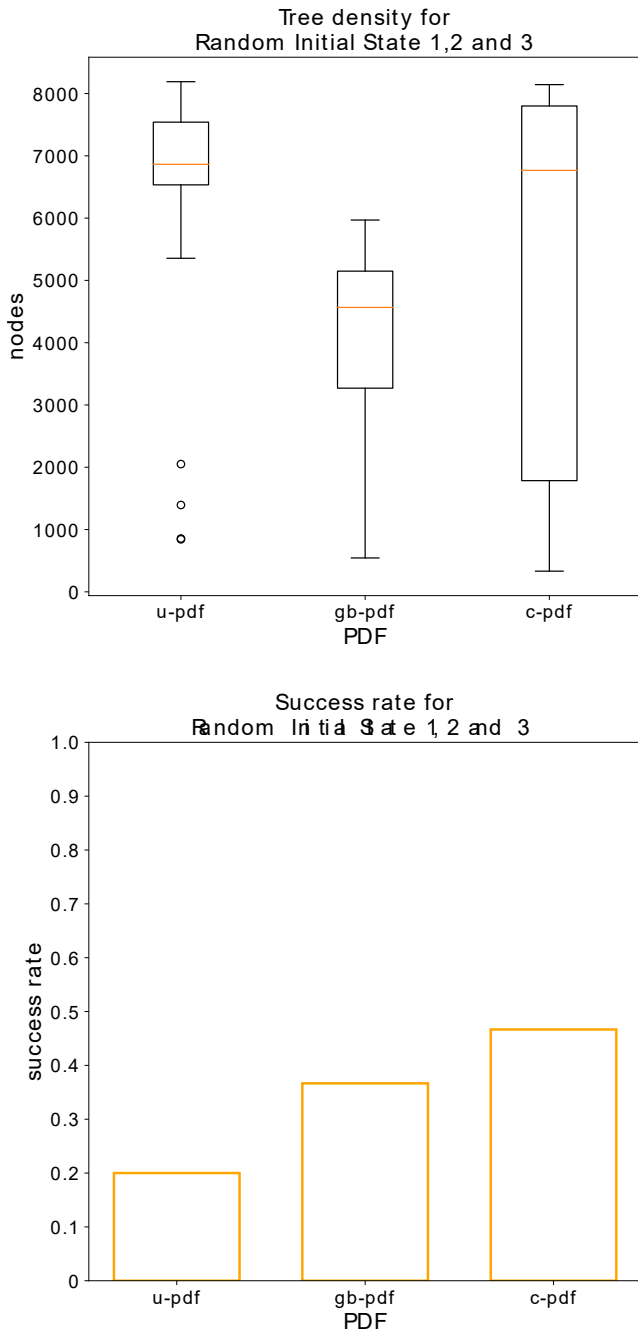


Fig. 10 For the task 4 comparative of tree density and success rate for three random initial state with a uniform, goal bias and custom PDF.

vertexes but a low increase in terms of meters (+6%) which means that the founding path has redundant actions we consider that an optimization process can easily reduce the number of vertexes.

In Figure 11, we can see the gradual tree growth. Please observe that when we use a custom PDF, we can rise the goal region in fewer vertexes, in the case shows for 1000 are enough to have a branch in the goal region aversely with the uniform and the goal bias PDF, the

tree has no branches outside of the room in the first quadrant. Moreover, for uniform PDF in 10,000 iterations, any vertex could get out of this quadrant. With the goal-bias PDF has branches in the first and third quadrant, but only a few branches begin to approach the goal region, while with the custom PDF, we have a branch in every quadrant and an important density of vertexes in the goal region, therefore a greater probability of finding a solution. In other words, the custom PDF explore and explode the workspace in a better way that the uniform and goal bias versions, an important characteristic in any search method.

5 Conclusions and future work

We presented a method for building a custom sampling distribution for random sampling planners. We show evidence that sampling from this custom probability density function improves the performance of the RRT planner with respect to uniform PDF and the RRT goal bias version, in the proposed tasks. We tested the method inside a virtual environment for three common tasks for autonomous vehicles and for a map with a classic problem of narrow passages. The results show that our method reduces the number of vertexes in the tree, decreases the computing time and increases the likelihood of finding a solution. From this point, we have evidence to support that a non-uniform PDF improves the performance of SBMPs when similar tasks have been solved, therefore, we can propose a methodology to infer this PDF.

The advantage of a random sampling algorithm is to deal with higher-dimensional spaces. For this reason, in a future work, we will test the proposed algorithm with a dynamic model of the car-like in tasks where it is necessary a high-velocity profile and likewise with more complex robots of more than three degrees of freedom. Finally, we also are interested in exploring techniques that use larger datasets such as deep-learning.

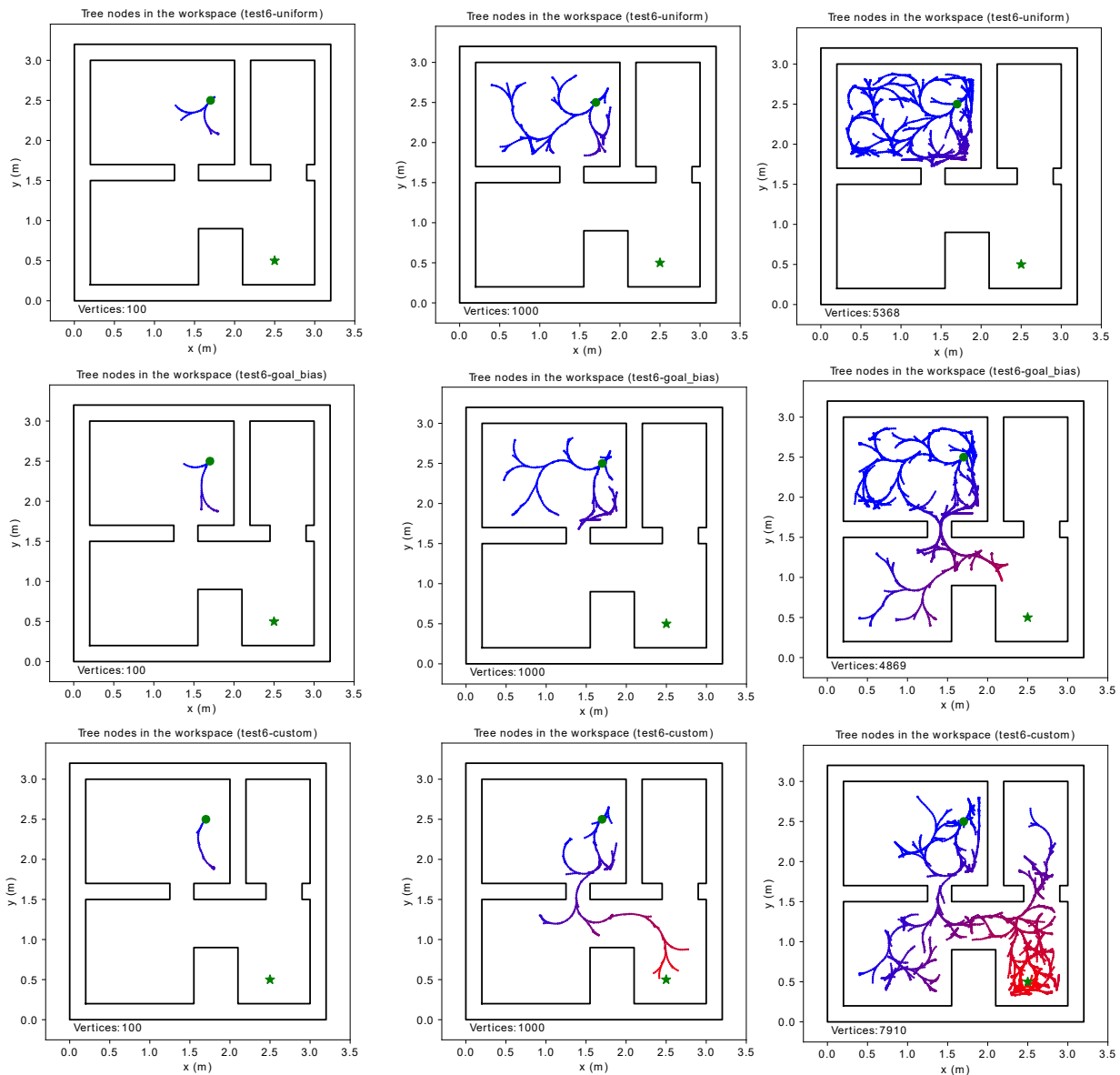


Fig. 11 Tree growth for the environment with narrow passages. From top to bottom task 4 with a uniform PDF, goal bias PDF and custom PDF. From left to right graph for 100, 1000 and all the vertices for each case with 10000 iterations. In blue are the vertices near to the initial state and in red color vertices close to the goal state. Figure best seen in color.

References

1. S. M. LaValle (2006) *Planning Algorithms*. Cambridge University Press
2. C. M. Bishop (2006) *Pattern Recognition and Machine Learning*. Springer, pp.528–530
3. P. Corke (2006) *Robotics, Vision and Control*, 2da ed. Springer, pp.109–111
4. L. E. Kavraki, P. Švestka, J-C. Latombe and M. H. Overmars (1996) Probabilistic RoadMaps for Path Planning in High-Dimensional Configuration Space. *IEEE Transactions on Robotics and Automation Control*, vol. 12, no. 4, pp. 566–580
5. S. M. LaValle and J. J. Kuffner (2001) Randomized Kinodynamic Planning. *The International Journal of Robotics Research*, vol. 20, no. 5, pp. 378–400
6. H-T. L. Chiang, J. Hsu, M. Fiser, L. Tapia and A. Faust RL-RRT: kinodynamic Motion Planning via Learning Reachability Estimators from RL Policies. *IEEE Robotics and Automation Letters*, PP. 1-1. 10.1109/LRA.2019.2931199
7. B. Ichter, J. Harrison and M. Pavone (2018) Learning Sampling Distribution for Motion Planning. *IEEE International Conference on Robotics and Automation*, pp. 7087–7094
8. Y-T. Lin (2006) The Gaussian PRM sampling for Dynamic Configuration Space. *International Conference on Control, Automation, Robotics and Vision*, Dec 5-8
9. D. Hsu, T. Jiang, J. Reif and Z. Sun (2002) The Bridge Test for Sampling Narrow Passage with Probabilistic Roadmap Planners. *IEEE International Conference on Robotics and Automation*, vol. 3
10. Y. Li, Z. Littlefield and E. Bekris (2016) “Asymptotically optimal sampling-based kinodynamic planning. *The Inter-*

- national Journal of Robotics Research*. vol. 35, no. 5, pp. 528–564
11. Steve LaValle (2002) Motion Strategy Library. <http://msl.cs.uiuc.edu/msl/>. Accessed 2019
 12. S. Karaman and E. Frazzooli (2011) Sampling-based algorithms for optimal motion planning. *International Journal of Robotic Research-IJRR*, vol. 30, no. 7, pp. 846–894
 13. A. Faust, K. Oslund, O. Ramirez, A. Francis, L. Tapia, M. Fiser and J. Davidson (2018) PRM-RL: Long-range Robotic Navigation Tasks by Combining Reinforcement Learning and Sampling-based Planning. *IEEE International Conference on Robotics and Automation*, pp. 5113–5120
 14. J. C. Latombe (1991) Robot motion planning. *Kluwer Academic Publisher*, Boston
 15. V. Boor, M. H. Overmars and A. Frank van der Stappen (1999) The Gaussian Sampling Strategy for Probabilistic Roadmap Planners. *IEEE International Conference on Robotics and Automation*, vol. 2, month. 05, pp. 1018–1023
 16. B. Burns and O. Brock (2007) Single-Query Motion Planning with Utility-Guided Random Trees. *IEEE International Conference on Robotics and Automation*, pp. 3307–3312
 17. J. P. van den Berg and M. H. Overmars (2005) Using Workspace information as a Guide to Non-uniform Sampling in Probabilistic Roadmap Planners. *The International Journal of Robotics Research*, pp. 1055–1071
 18. H. Kurniawati and D. Hsu (2004) Workspace Importance for Probabilistic Roadmap Planning. *IEEE International Conference on Intelligence Robots and Systems*, vol. 2, pp. 1618–1623
 19. M. Zucker, J. Kuffner and J. A. Bagnell (2008) Adaptive workspace biasing for sampling-based planners. *IEEE International Conference on Robotics and Automation*, pp. 3757–3762
 20. A. Yershova, L. Jaillet, T. Siméon and S.M. LaValle (2005) Dynamic-Domain RRTs: Efficient Exploration by Controlling the Sampling Domain. *IEEE International Conference on Robotics and Automation*, pp. 3856–3861
 21. D. Berenson, P. Abbel and K. Goldberg (2005) A Robot Path Planning Framework that learns from Experience. *IEEE International Conference on Robotics and Automation*, pp. 3671–3687
 22. J. D. Gammell, S. S. Srinivasa and T. D. Barfoot (2015) Batch Informed Trees (BIT*): Sampling-based Optimal Planning via the Heuristically Guided Search of Implicit Random Geometric Graphs. *IEEE International Conference on Robotics and Automation*, pp. 3067–3074
 23. D. Coleman, I. A. Sucas, M. Moll, K. Okada and N. Correll (2015) Experience-Based Planning with Sparse Roadmap Spanners. *IEEE International Conference on Robotics and Automation*,
 24. S. M. LaValle (1998) Rapidly-Exploring Random Trees: A New Tool for Path Planning *Computer Science Dept*, Iowa State University
 25. B. Ichter and M. Pavone (2019) Robot Motion Planning in Learned Latent Spaces. *IEEE Robotic and Automation Letters*
 26. D. González, J. Pérez, V. Milanés and F. Nashashibi (2015) A Review of Motion Planning Techniques for Automated Vehicles. *IEEE Transactions on Intelligent Transportation Systems*
 27. M. H. Korayem, M. Nazemizadeh and H. R. Nohooji (2014) Optimal point-to-point motion planning of non-holonomic mobile robots in the presence of multiple obstacles. *Journal of the Brazilian Society of Mechanical Sciences and Engineering*
 28. L. Janson, E. Schmerling, A. Clark and M. Pavone (2015) Fast Marching Tree: A Fast Marching Sampling-Based Method For Optimal Motion Planning in Many Dimensions. *Int. J. Robot. Res*
 29. A. H. Qureshi, A. Simeonov M. J. Bency and M. C. Yip (2019) Motion Planning Networks: Bridging the Gap Between Learning-based and Classical Motion Planners *IEEE International Conference on Robotics and Automation*
 30. P. K. Mohanty and H. S. Dewang (2021) A smart path planner for wheeled mobile robots using adaptive particle swarm optimization *Journal of the Brazilian Society of Mechanical Sciences and Engineering*